Mapping Interactions between the Catalytic Domain of Resolvase and Its DNA Substrate Using Cysteine-Coupled EDTA–Iron†

Joan M. Mazzarelli,‡ Mario R. Ermácora,‡,§ Robert O. Fox,‡,§ and Nigel D. F. Grindley*,‡

Department of Molecular Biophysics and Biochemistry and Howard Hughes Medical Institute, Yale University, New Haven, Connecticut 06510

Received October 27, 1992; Revised Manuscript Received December 18, 1992

ABSTRACT: Single cysteine-substituted mutants of γδ resolvase have been covalently modified using a novel sulfhydryl-specific EDTA derivative, EDTA–2-aminoethyl 2-pyridyl disulfide (EPD). Iron, chelated by the coupled EDTA and in the presence of reducing agent, generates reactive oxygen species that result in localized cleavage of the DNA to which resolvase is bound. The procedure provides valuable information on two fronts. First, it allows the identification of regions or surfaces of the protein that are in close proximity to DNA even though they may not be part of the DNA-binding domain. Second, it allows identification of the portions of DNA that are closest to each EDTA-derivatized cysteine, since the DNA cleavages observed are highly localized and their efficiency drops rapidly as a function of the distance between the EDTA–Fe complex and the deoxyribose target. We have used the procedure to investigate the interaction of γδ resolvase with the three DNA binding sites that constitute its recombination substrate, *res*. The data indicate that the two N-terminal domains of a resolvase dimer interact symmetrically with site I, which contains the recombination cross-over point, but asymmetrically with the accessory sites, II and III. The patterns of DNA cleavage obtained with several different EDTA-coupled mutants have enabled us to propose a model for the interaction between resolvase and site I.

Many proteins that act upon nucleic acids carry out their catalytic activities via large specialized nucleoprotein structures which guide and direct the nucleic acid transactions. Such nucleoprotein structures are involved in the initiation of DNA replication, site-specific recombination, transposition intermediates, translation, and RNA processing (Echols, 1986; Echols, 1990; Landy, 1989; Mizuuchi, 1992; Lührmann, 1988; Noller, 1991). Currently, biophysical methods available for determining the structures of these large nucleoprotein complexes are limited due to their molecular size. The further development of tools such as photochemical cross-linking (Williams & Konigsberg, 1991) or biochemical footprinting methods (Dervan, 1991; Dixon et al., 1991) is needed to probe the structures of nucleoprotein complexes in order to establish which regions of the protein are critical for function or come in close contact with specific regions of the nucleic acid.

Site-specific recombination mediated by γδ resolvase occurs within a synaptic complex consisting of two copies of the recombination substrate, *res*, and at least six dimers of resolvase [for a review, see Hatfull and Grindley (1988)]. The 21-kDa resolvase protein is encoded by the transposon γδ, a member of the Tn3 family of transposable elements. The recombinase catalyzes the resolution of cointegrates, replicons carrying two copies of γδ in direct orientation. The resolvase interacts with *res* DNA which is located between the *tnpA* and *tnpR* genes of the transposon (Figure 1). An individual *res* site contains three binding sites, each for a dimer of resolvase. Each binding site consists of two imperfectly conserved 12 base pair binding sequences in inverted orientation separated by a variable spacer: four base pairs in site I, ten base pairs in site II, and one base pair in site III (Figure 1; Grindley et al., 1982; Rimphanitchayakit et al., 1989). The recombinational cross-over point lies at the center of site I (Reed & Grindley, 1981).

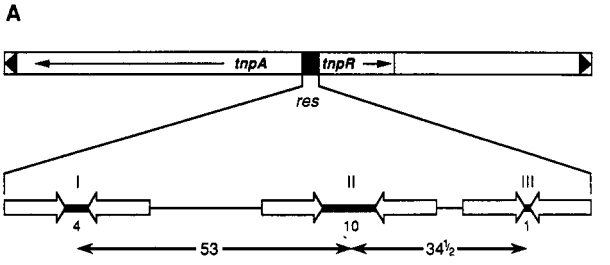

FIGURE 1: γδ transposon showing the *res* site. The upper portion shows the entire γδ transposon with *tnpR* and *tnpA* genes transcribed in the direction of the arrows. Below is a schematic of *res*. I, II, and III indicate the three resolvase binding sites, each consisting of a pair of inverted 12-bp sequences (open arrows) recognized by the C-terminal doman of resolvase. Numbers indicate length (in base pairs) of internal spacers (heavy lines) and the center–center separation of sites I, II, and III.

γδ resolvase has two domains, a 140 amino acid N-terminal domain and a 43 amino acid C-terminal domain (Abdel-Meguid et al., 1984). The small domain interacts specifically with adjacent major and minor grooves of the individual 12-bp binding sequences of *res* and, on the basis of sequence homology, appears to contain a helix–turn–helix DNA-binding motif (Abdel-Meguid et al., 1984; Rimphanitchayakit et al., 1989; Rimphanitchayakit & Grindley, 1990; Graham & Dervan, 1990). The large domain of resolvase contains the recombinational active site including the catalytic serine residue, Ser-10 (Reed & Moser, 1984; Hatfull & Grindley, 1986). It is also responsible for subunit dimerization and facilitates cooperative interactions between resolvase dimers bound to *res* (Hughes et al., 1990).

The crystal structure of the first 120 amino acids of the catalytic domain of resolvase has provided information about

† This work was supported by NIH Grant GM28470 to N.D.F.G. and by the Howard Hughes Medical Institute (R.O.F.). Joan Mazzarelli was supported by a Brown-Coxe Postdoctoral Fellowship from Yale University School of Medicine for part of this work.

* Address correspondence to this author.
‡ Department of Molecular Biophysics and Biochemistry.
§ Howard Hughes Medical Institute.

0006-2960/93/0432-2979$04.00/0

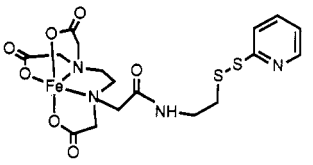

FIGURE 2: EDTA–2-aminoethyl 2-pyridyl disulfide, EPD. Disulfide exchange allows the coupling of the EDTA–2-aminoethyl moiety to any free thiol—in our case, cysteine residues in mutants of resolvase.

protein–protein interactions that occur in the formation of resolvase–*res* nucleoprotein complexes (Sanderson et al., 1990; Hughes et al., 1990), but it has proved very difficult to model *res* DNA onto the crystal structure since the DNA-binding domain is absent. Two alternative dimeric arrangements of the resolvase catalytic domain are visible in the crystal structure; these are referred to as the 1,2 and 2,3 dimers. Cysteine and other substitutions made at these alternative interfaces have revealed that it is the 1,2 dimer of resolvase that binds each individual site in *res* (Hughes et al., 1993). However, in the crystal structure, the Ser-10 residues of the 1,2 dimer are separated by more than 30 Å, too far apart to interact readily with the phosphodiester bonds cleaved during recombination without substantial distortion of DNA or conformational adjustments to the protein dimer.

To gain additional insight into the protein–DNA interactions that occur in the resolvase–*res* nucleoprotein complexes, we have used a novel approach to determine which parts of the catalytic domain of resolvase are near the *res* DNA. Cysteine residues of various single cysteine-substituted mutants of resolvase (the wild-type protein lacks cysteine) were coupled to EDTA using a sulfhydryl-specific reagent, EDTA–2-aminoethyl 2-pyridyl disulfide, EPD (Figure 2) (Ermácora et al., 1992). Incorporation of the EDTA moiety at single amino acid residues in a protein allows the position of those residues in a protein–DNA complex to be mapped relative to the DNA base pairs. Iron is chelated by the EDTA moiety of the protein and, upon the addition of a reducing agent such as ascorbate, reactive oxygen species, probably hydroxyl radicals, are generated in solution; these react with sugars of the DNA backbone, cleaving the DNA (Tullius, 1989). In previous work, coupling EDTA–Fe to DNA-binding proteins has been limited to the incorporation of the EDTA moiety at the C or N terminus of a synthetic sequence-specific DNA-binding peptide (Sluka et al., 1987, 1990a,b; Mack et al., 1990; Graham & Dervan, 1990; Oakley & Dervan, 1990; Dervan, 1991). The sulfhydryl-modifying reagent, EPD, however, makes this approach much simpler and allows EDTA derivatization of any position in a protein where a cysteine residue exists (or is placed by site-directed mutagenesis). Other DNA-binding proteins, the *trp* repressor (Chen & Sigman, 1987), the λ phage cro protein (Bruice et al., 1990), and the catabolite gene activator protein, CAP (Ebright et al., 1990), have been converted into site-specific nucleases using sulfhydryl-specific 1,10-phenanthroline derivatives. The Fe–EDTA moiety used in the studies described here is hydrophilic and thus does not rely on hydrophobic interactions for DNA cleavage. It also has no preference for the minor groove of DNA as is seen with 1,10-phenanthroline (Kuwabara et al., 1986; Sigman, 1986; Sigman et al., 1991). During the preparation of the manuscript we learned that the EPD reagent has been made by a different synthetic route and applied to the study of the DNA interactions of both CAP and Cro by Ebright and his colleagues (Ebright et al., 1992).

EXPERIMENTAL PROCEDURES

Preparation of Cysteine Mutants of γδ Resolvase. Cysteine-substituted mutants of γδ resolvase (Hatfull et al., 1989) were purified as described (Reed, 1981). The large domain of the S10C mutant was overexpressed from pJM1. This plasmid was created using a 2965 base pair *Pst*I fragment obtained from pGH160, the plasmid encoding the S10C mutant (Hatfull & Grindley, 1986), and a 3376 base pair *Pst*I fragment obtained from pGH288, the large fragment overproducer. Purification of the large fragment of resolvase is described elsewhere (Hatfull et al., 1989).

Derivatization of γδ Resolvase Cysteine Mutants. All the mutants except S10C were derivatized using EPD complexed with iron; this eliminated the need to add ferrous sulfate and sodium citrate later. For historical reasons, S10C was derivatized using uncomplexed EPD and iron was added subsequently. Prior to derivatization, each resolvase mutant was precipitated by dialysis against 20 mM Tris-HCl, pH 7.4, 20 mM $MgCl_2$, 1 mM DTT. The majority of the DTT was then removed by dialysis against a buffer of Tris-HCl, pH 7.4, or MES, pH 6.0. Each cysteine mutant (2–3 mg) was reacted in 100 mM Tris-HCl, pH 7.3, 1 M NaCl at 4 °C; 3 mM EPD or its iron complex (Ermácora et al., 1992) was added to give a 2-fold molar excess over resolvase monomer, and the reaction was allowed to proceed for 20 h at 4 °C. Each protein was separated from low molecular weight materials (unreacted EPD and 2-thiopyridone) using a gel filtration column (1.0 × 18.0 cm containing Bio-Gel P4, 100–200 mesh, Bio-Rad) equilibrated in 100 mM Tris-HCl, pH 7.3, 1 M NaCl. Solutions had been treated with Chelex 100, (100–200 mesh, Bio-Rad) to remove trace divalent cations. In the case of S10C, the protein–EDTA adduct was complexed with iron. A 2-fold molar excess over resolvase monomer of ferrous sulfate (5 mM in deaerated water) was added to the protein solution and, after 20 min at 4 °C, 3 μL of 40 mM sodium citrate was added to scavenge any uncomplexed iron. Underivatized S10C was treated similarly with iron and citrate as a control.

Determination of Extent of Derivatization. Each derivatized cysteine mutant was lyophilized, oxidized with performic acid (Hirs, 1967), and hydrolyzed (6 N HCl, 110 °C, 20 h) (Moore & Stein, 1963). Amino acid analysis was performed on a 7300 Beckman autoanalyzer with ninhydrin detection. Taurine and cysteic acid resulted from the oxidation of, respectively, the derivatized and underivatized portions of the protein. The proportion of each mutant that was derivatized was then calculated from the ratio of taurine to cysteic acid (Ermácora et al., 1992); this varied from 40% (K65C) to 90% (E102C).

DNA Cleavage Reactions. Binding reactions (10 μL) containing 20 mM Tris-HCl, pH 8.0, 100 mM NaCl, 100 μg/mL sonicated calf thymus DNA, ^{32}P-labeled DNA fragment, and derivatized cysteine mutant were incubated at 37 °C for 10 min. One microliter of a solution of 300 mM Tris-HCl, pH 7.0, 300 mM sodium ascorbate, and 1 M NaCl was added, and the reaction was allowed to proceed for 1 h at 22 °C. The reaction was stopped by ethanol precipitation. The pellets were washed with 70% ethanol, dried, and suspended in 2 μL of formamide dyes. The samples were heated to 90 °C and then subjected to denaturing polyacrylamide gel electrophoresis on a 6, 8, or 10% gel. To assist in the quantitation of cleavages, autoradiograms were scanned with an LKB Ultroscan XL laser densitometer.

Hydroxyl Radical Footprinting. Five microliters of a solution containing equal volumes of 10 mM $Fe(NH_4)_2(SO_4)_2$

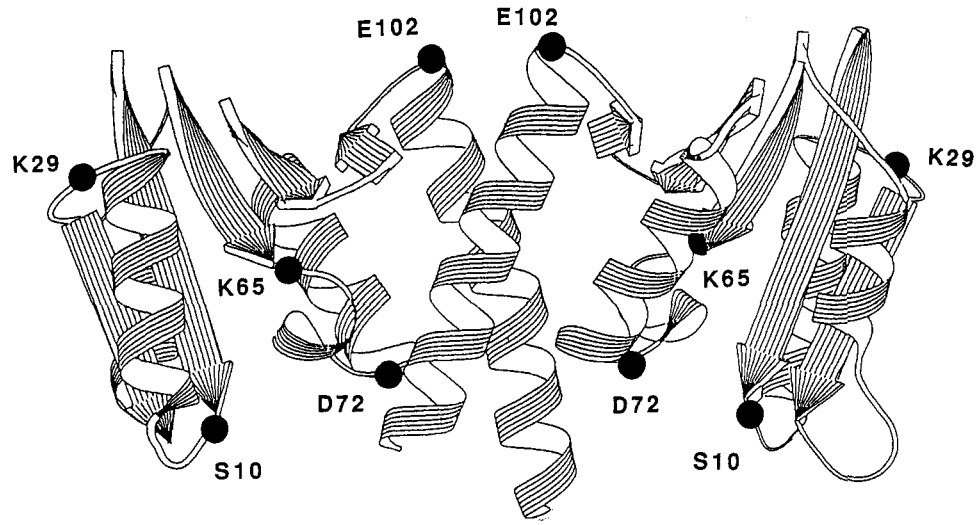

FIGURE 3: Representation of the α-carbon backbone of the 1,2 dimer of the resolvase catalytic domain (amino acids 1–120 are shown) (Sanderson et al., 1990; figure contributed by P. Rice and T. A. Steitz). The positions of the wild-type amino acids changed to cysteines and then modified with EPD are noted.

and 20 mM EDTA was added to 25 μL of 3% v/v H_2O_2, 5 μL of 100 mM L-ascorbic acid, and 15 μL of distilled water; 10 μL of this Fe–EDTA solution was added to each binding reaction (Hatfull et al., 1987). Prior to the addition of the Fe–EDTA solution, the binding reactions (90 μL) were incubated for 10 min at 37 °C. The Fe–EDTA solution was then added and the incubation continued for 2 min. The 100-μL binding reactions contained 0, 8, 80, or 240 nM resolvase, 20 mM Tris-HCl, pH 7.5, 5 mM $MgCl_2$, 100 mM NaCl, ^{32}P-labeled DNA (containing either sites I, II, or III), 100 μg/mL BSA, 10 μg/mL sonicated calf thymus DNA, 50 μM $Fe(NH_4)_2(SO_4)_2$, 100 μM EDTA, 0.15% v/v H_2O_2, and 1 mM ascorbate. To terminate the DNA cleavage reaction, 10 μL of thiourea (100 mM) was added, and the reaction was frozen on dry ice. After the reaction was thawed, 13 μL of 3 M sodium acetate, 2 μL of 0.5 M EDTA, and 350 μL of ethanol were added, and the DNA was precipitated. The DNA pellet was washed with 70% ethanol, dried, and resuspended in formamide dyes.

Plasmids and DNA Fragments. The DNA fragments used in the footprinting assays, containing sites I, II, and III of *res*, were obtained individually from pVR90. The site I fragment was a 127 base pair *Sal*I–*Hin*dIII fragment. The site II fragment was an 80 base pair *Asp*718–*Bam*HI fragment and the site III was a 187 base pair *Bam*HI–*Sal*I fragment. DNA fragments were end-labeled with ^{32}P either by consecutive treatments with calf alkaline phosphatase and T4 polynucleotide kinase or by filling using an *exo*$^-$ mutant of DNA polymerase I Klenow fragment (a gift from Vicky Derbyshire). The ^{32}P-labeled fragments were purified by polyacrylamide gel electrophoresis. The A + G markers were generated by chemical sequencing methods (Maxam & Gilbert, 1980).

Binding Assay. Binding of the cysteine mutants and the partially derivatized proteins to sites I, II, and III of *res* was detected using native polyacrylamide electrophoresis essentially as described by Hatfull et al. (1986).

RESULTS

Positions Selected for EDTA Derivatization

Wild-type γδ resolvase contains no cysteine residues. The cysteine-substituted mutants of resolvase, S10C, K29C, K65C, D72C, and E102C, were selected for derivatization on the basis of inspection of the three-dimensional structure of the catalytic domain of the protein (Sanderson et al., 1990) (Figure 3). The residues Ser-10, Asp-72, and Lys-65 are located near to one another on the surface of the protein thought to be involved in the binding of the cross-over site of *res*. Ser-10 appears to be the catalytic serine of resolvase that is covalently linked to the 5′ phosphate of the cleaved cross-over site in a recombinational intermediate (Reed & Moser, 1984; Hatfull & Grindley, 1986). In the asymmetric unit of crystals of the catalytic domain of resolvase (Sanderson et al., 1990), there are two dimers referred to as the 1,2 and 2,3 dimers. In the E102C mutant, the cysteine substitution is located at the amino terminus of an α helix which is part of the 1,2 dimer interface in the crystal structure. The cysteine of the K29C mutant is located on another surface of the protein close to the 2,3 dimer interface. The N-terminal domain of resolvase containing the S10C mutation was also derivatized and used as a control for DNA cleavage. This mutant lacks the carboxy-terminal domain of the protein and so is unable to bind DNA (Abdel-Meguid et al., 1984).

DNA Cleavage by the EDTA-Derivatized Cysteine Mutants

DNA-Cleaving Properties of Derivatized Mutants on Site I. Of the five EDTA-derivatized mutants, three, S10C, K65C, and D72C, produced specific DNA cleavages on the fragment containing site I. The primary cleavages for these derivatized mutants were located within the internal spacer region of site I on the base pairs located near the cross-over point (Figure 4A,B). Secondary cleavages (those of lower relative intensity) are also visible on the site I fragment adjacent to the spacer region. In control reactions using S10C (underivatized) and citrate–iron, no DNA cleavage was observed. When the symmetrical DNA cleavage patterns of the three mutants are compared, it is clear that there is considerable overlap in cleavage sites. However, there are also readily discernible differences especially in the relative intensities of particular cleavages (Figure 4). Hydroxyl radicals generated by the modified S10C mutant primarily attacked base pairs adjacent to the cross-over point, especially the two nucleotides of the 3′ overhang formed by resolvase-mediated cleavage during recombination. The most intense cleavages resulting from the derivatized D72C and K65C proteins were shifted respectively one and two bases in the 3′ direction on each strand relative to those of the S10C mutant (Figure 4B). The

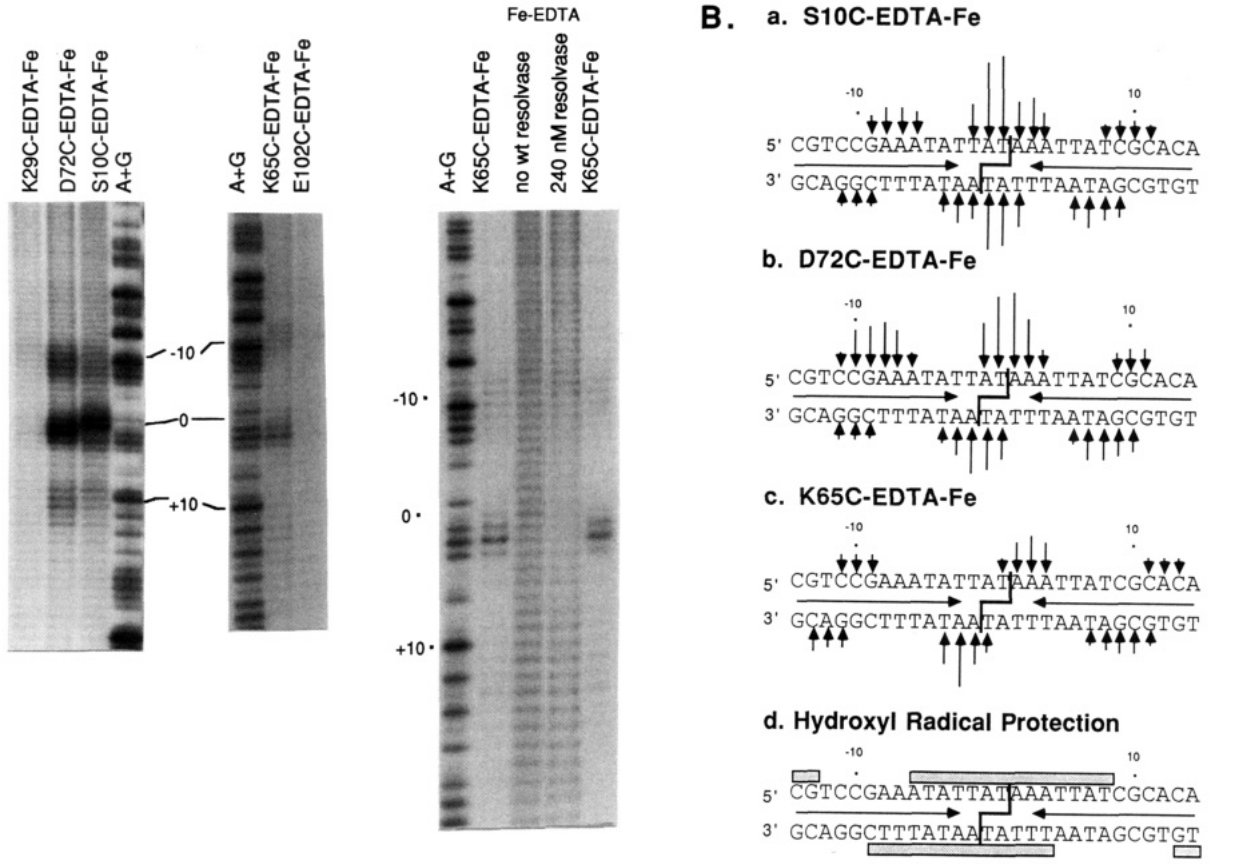

FIGURE 4: DNA cleavages within site I produced by EDTA–Fe derivatives of resolvase mutants S10C, D72C, K29C, K65C, and E102C. (A, left) Autoradiograms of 8% polyacrylamide gels displaying top strand data. A hydroxyl radical footprint of wild-type resolvase is also shown as a control (lanes marked Fe–EDTA). Numbers indicate nucleotide positions in site I relative to the center of site (=0). (B, right) Summary of site I data. Vertical arrows represent the extent of site-specific cleavage generated by (a) S10C–EDTA–Fe, (b) D72C–EDTA–Fe, and (c) K65C–EDTA–Fe. The horizontal arrows represent the inverted 12-bp sequences recognized by the C-terminal domain of resolvase. (d) Hydroxyl radical footprinting: shaded bars show regions protected from hydroxyl radicals by wild-type resolvase.

implications of the cleavage patterns resulting from these three derivatized mutants will be analyzed in the Discussion. Neither E102C nor K29C, when derivatized with EDTA–Fe, produced strong cleavages on the site I fragment although in both cases some very weak secondary cleavages could be seen (Figure 4A). As indicated below, we believe that both these proteins bind to site I and suggest that their failure to cleave efficiently within site I results from remote positioning of the EDTA–Fe moiety.

The different, but highly reproducible, cleavage patterns seen with each derivatized resolvase argue strongly that we are looking at the effects of locally generated hydroxyl radicals. As an additional control, Figure 4 shows a footprint of wild-type resolvase at site I produced by EDTA–Fe in solution. A block of protection spans the center of site I right across the positions at which the most intense cleavages were seen with the EDTA derivatives of S10C, D72C, and K65C.

DNA-Cleaving Properties of Derivatized Mutants on Fragments Containing Site II or III. Three of the five EDTA-derivatized resolvase mutants produced site-specific DNA cleavage on fragments containing site II or III of *res* (Figure 5). In contrast to the symmetric cleavage patterns observed at site I, those at sites II and III were distinctly asymmetrical. At site II the three derivatized mutants S10C, D72C, and E102C preferentially cleaved the left half of the site. Moreover, those cleavages obtained within the right half (only with S10C and D72C) were not centered at the positions symmetrical to those in the left half but, rather, were shifted about 2 bp away from the center toward the right half of site II (Figure 5A,B). These results suggest that the resolvase–site II interaction is unexpectedly asymmetric with the left half in closer contact with a resolvase catalytic domain (of the bound 1,2 dimer) than is the right half. The displacement of cleavages from the dyad of the site suggests that the resolvase-induced bend in site II (Salvo & Grindley, 1988) may be asymmetric and not centered on the dyad.

Site III was cleaved by the same three EDTA-derivatized resolvase mutants, S10C, D72C, and E102C, as site II, and again a distinct asymmetry was observed (Figure 5C). Both S10C and D72C resulted in cleavages predominantly in the left half of the site. By contrast, the derivatized E102C cleaved exclusively the right half of the site. As with site II, these results indicate that the resolvase–site III interaction is asymmetric with each half of the site being in close proximity to a different region of the catalytic domains of the bound resolvase dimer.

Binding Affinities of the Cysteine Mutants and the Derivatized Proteins

The inability of a derivatized cysteine mutant to produce hydroxyl radical cleavage could result from two trivial reasons—(i) insufficient derivatization or (ii) inability of derivatized protein to bind *res* DNA—or, more meaningfully, from distant position of the EDTA moiety with respect to the DNA, possibly combined with protection of the nearest segment of DNA by another portion of the protein. Three derivatized resolvase mutants, K65C, K29C, and E102C, failed to cleave one or more of the binding sites in *res*. Native and EDTA-derivatized preparations of all three mutants were

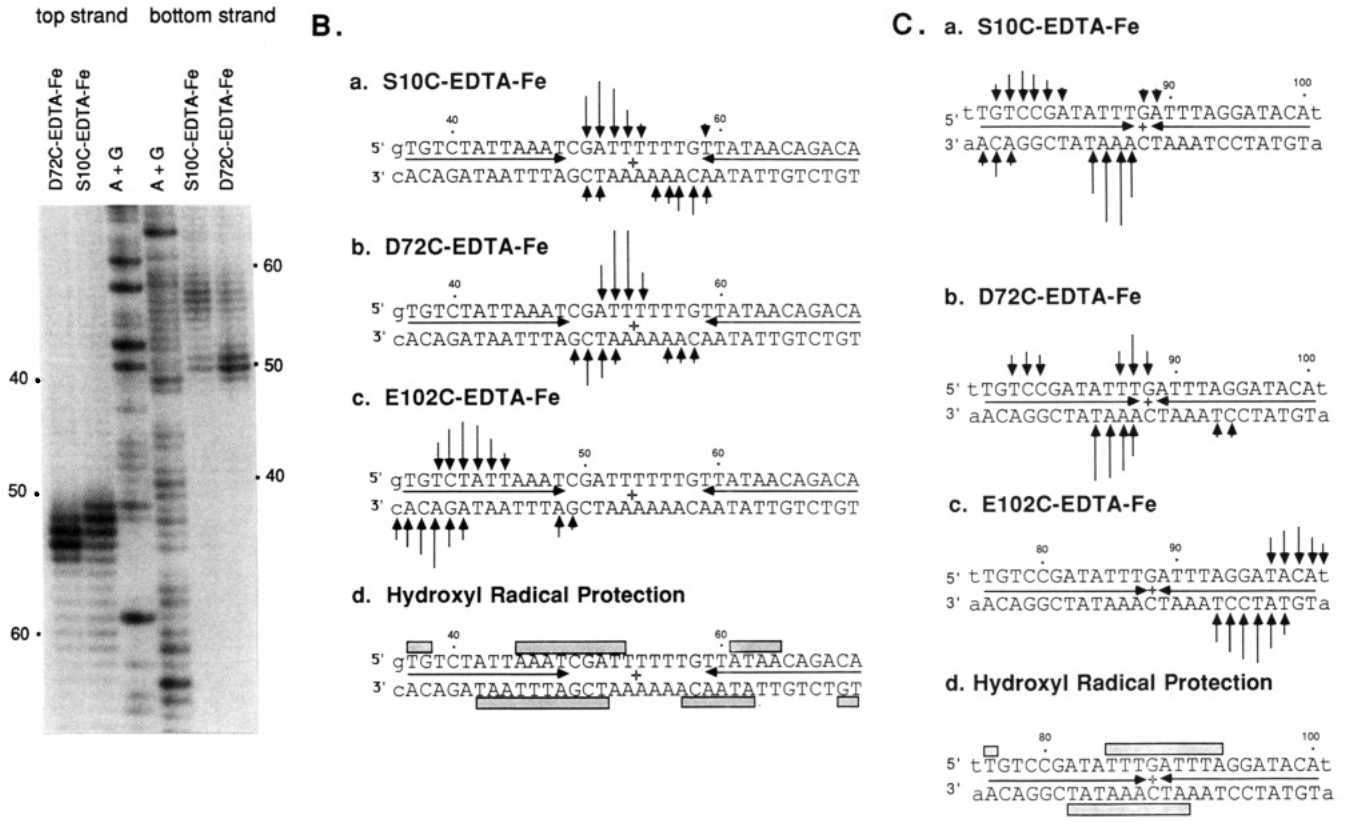

FIGURE 5: DNA cleavages within sites II and III. (A, left) Autoradiogram of an 8% polyacrylamide gel which reveals the site-specific cleavage produced by S10C–EDTA–Fe and D72C–EDTA–Fe on an 80-bp fragment containing site II. Numbers indicate the nucleotide positions relative to the center of site I (=0). (B, middle) Summary of site II data. For details see legend to Figure 4B. The plus sign indicates the dyad of the binding site. (C, right) Summary of site III data.

assayed for DNA binding to the individual binding sites (data not shown). K65C bound efficiently only to site I. This result suggests that the inability of K65C–EDTA–Fe to cleave sites II and III is a direct consequence of poor DNA binding to these subsites. The K29C and E102C proteins both bound to all three sites. However, since EDTA-derivatization was never 100%, it is difficult to rule out the possibility that the presence of the EDTA–Fe moiety reduces DNA affinity. In the case of E102C, since the derivatized protein cleaves both sites II and III and bound all three sites with similar efficiency, we consider it highly likely that the lack of strong cleavage within site I is a result of remote positioning of the hydroxyl radical sources. A similar explanation is most likely for K29C, since the protein was determined by amino acid analysis to be 50% derivatized; however, its failure to produce cleavages within any of the three sites tempers this conclusion since derivatization may selectively reduce DNA affinity.

DISCUSSION

EPD: A Tool for the Study of Protein–DNA Interactions. The sulfhydryl-specific EDTA reagent, EPD, was initially developed by Ermácora et al. (1992) as a tool for the study of protein folding. In this paper we have demonstrated its utility for studying protein–DNA interactions. As an aid to modeling the complexes formed between $\gamma\delta$ resolvase and its DNA binding sites, we have combined the cysteine-coupling property of EPD with a collection of cysteine-substituted resolvases (Hatfull et al., 1989). In the presence of iron and ascorbate, hydroxyl radicals generated at the EDTA–cysteine positions result in localized cleavage of bound DNA. Our aim was 2-fold: (i) to identify regions of the resolvase catalytic domain that, in resolvase–DNA complexes, were in close proximity to DNA, and (ii) to identify the specific nucleotides approached most closely by these regions.

Several aspects of our data suggest that this approach can be very informative. First, resolvase–EDTA derivatives that effect iron-dependent DNA cleavage do so in a highly localized manner with only a limited number of nucleotide positions being attacked efficiently. Second, a relatively small change in the position of the amino acid residue to which EDTA is coupled results in a distinctive change in the hydroxyl radical cleavage pattern (see, for example, the data for cleavage of site I by S10C and D72C in which the α-carbons of the derivatized residues are about 12 Å apart). Third, only a subset of the EDTA-coupled resolvase mutants that bound DNA produced DNA cleavages. Finally, the hydroxyl radical cleavages are not simply a localized subset of those cleavages obtained in a conventional EDTA–Fe footprinting experiment. Rather, the most intense cleavages within site I produced by the EDTA derivatives of S10C, D72C, and K65C lie within a region normally protected from hydroxyl radical attack by wild-type resolvase and thus presumably in close contact with it (see Figure 4). Overall, these observations suggest that DNA cleavage is limited to the immediate vicinity of the EDTA-coupled residue and occurs only when this residue lies close to the DNA. The failure of K29C–EDTA to promote DNA cleavage, even though derivatization was efficient and DNA binding appeared to be unaffected, is entirely consistent with the fact that position 29 is on a surface of resolvase well removed from the presumed catalytic surface that contains residues Ser-10, Lys-65, and Asp-72 (Sanderson et al., 1990; see Figure 3).

Cleavage Patterns in Site I Suggest a Model for the Resolvase–Site I Interaction. EDTA derivatives of the mutants K65C, S10C, and D72C produced symmetrical DNA

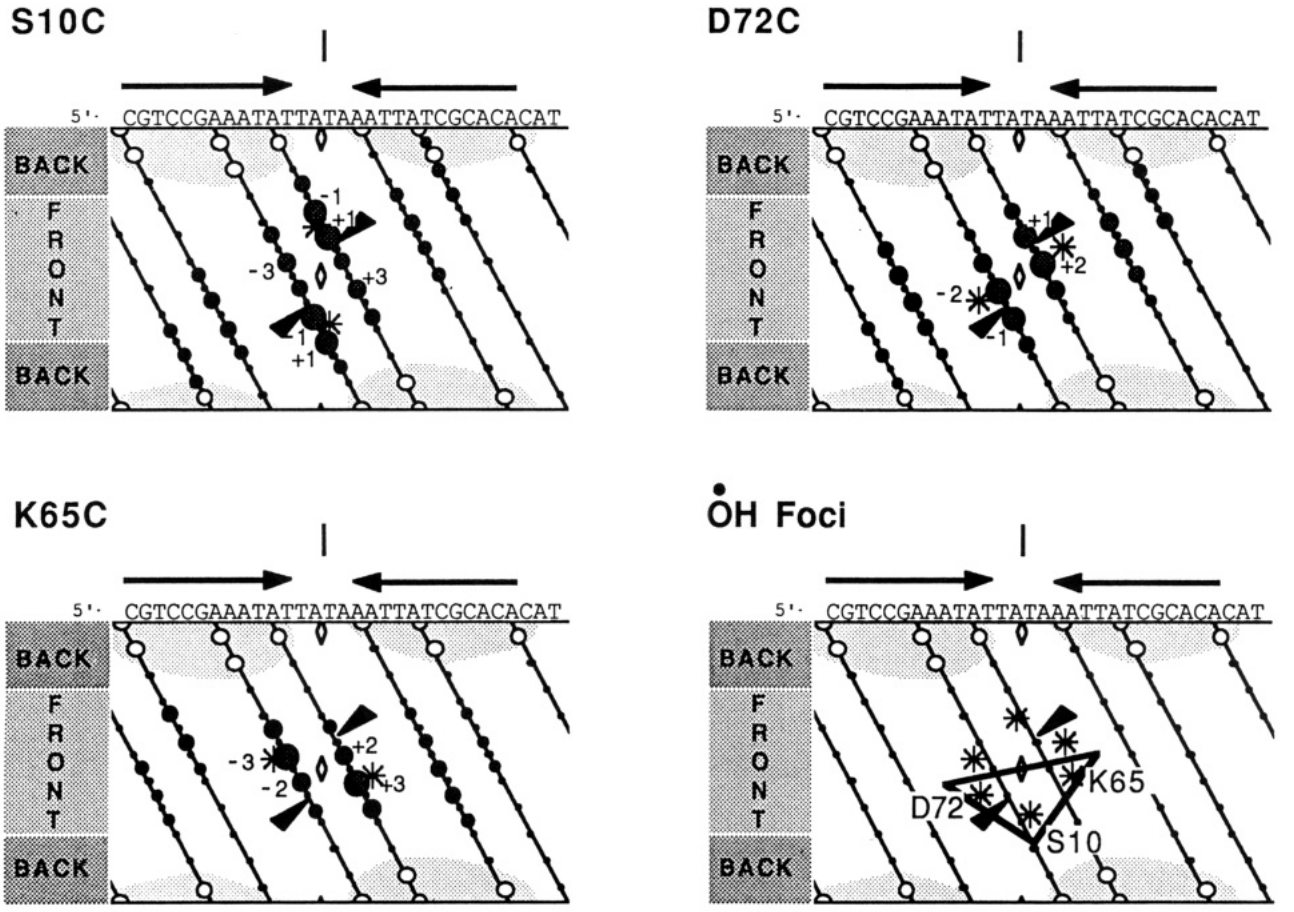

FIGURE 6: Planar DNA representation of site I DNA showing hydroxyl radical cleavages produced by the derivatized proteins. The DNA sequence is for the top strand of *res*; the horizontal arrows indicate the 12-bp binding sequences. The DNA helix is represented as a cylinder split down one one side and unfolded; a helical repeat of 10.5 base pairs is assumed. Black dots represent the phosphates of the sugar–phosphate backbone. Black arrowheads indicate the positions of strand breakage during recombination. The diamond symbols in the major and minor grooves indicate the dyad axis of the binding site. The shaded areas represent the areas contacted by the C-terminal domain of resolvase; the open circles are phosphates that when ethylated inhibit C-terminal domain binding. The solid circles represent positions of deoxyribose moieties attacked by hydroxyl radicals from each EDTA-modified resolvase; the size of the symbol indicates the efficiency of attack. Asterisks represent the approximate placement of the EDTA–Fe moieties of each dimer (the foci of hydroxyl radicals).

cleavages in the center of site I. The positions of cleavage reveal that this particular surface of the catalytic domain appears to come close to the cross-over site of *res* even on linear DNA fragments that contain only binding site I. This is an important observation since it suggests that juxtaposition of the catalytic site and DNA cleavage point does not depend on assembly of the synaptic complex but, rather, is established when resolvase binds to site I. This supports and extends the conclusions of Dröge et al. (1991), who showed that, with respect to the entire *res* site, resolvase operates catalytically in cis (that is, the resolvase initially bound to one *res* of a cointegrate substrate preferentially cleaves the cross-over point of that *res*).

The specific patterns of cleavage obtained with each of the three derivatized resolvase mutants can be used to deduce the approximate position of closest approach of the three relevant residues to the cross-over region. If the data for each derivatized mutant, S10C, K65C, and D72C, are plotted on a planar representation of site I DNA (Figure 6), it appears that the cleavages can be explained as resulting from two centers, or foci, of hydroxyl radical generation. Clearly, there is some uncertainty in the location of these foci; however, we have positioned them as shown in Figure 6 for the following reasons. [In the arguments that follow we have ignored the DNA distortion at the center of site I induced by resolvase binding (Hatfull et al., 1987) since we do now know its precise nature; however, we do not believe that this significantly affects our conclusions.] In the case of the derivatized S10C data, the most efficient cleavages are at positions +1 and –1 on the top strand and at –1 and +1 on the bottom strand, but each of these pairs appears to belong to a separate cluster of cleavages. First, the strongest cleavages are not directly across the minor groove from each other. In addition, since cleavage at +3 (top strand) occurs more readily than at the adjacent +2, we argue that the former is part of the cluster centered on the bottom strand positions +1,–1, rather than on the top strand positions. Secondary cleavages of the +1,–1 top strand cluster appear to include (in decreasing order of efficiency) those at –3, –4, and +7 all on the bottom strand. Because the –3 cleavage (across the minor groove from +1) on the bottom strand is more intense than that at +7 (directly across the the major groove), we suggest that the source of hydroxyl radicals is above the minor groove or the sugar–phosphate backbone of the top strand. A similar set of arguments applies to the cluster centered on position –1,+1 (bottom strand). The D72C data are a little more complicated. The most intense cleavages (at +2, top strand; and –2, bottom strand) are (in B-form DNA) right across the minor groove from one another and, thus, could result from a single source of hydroxyl radicals. However, a dimer of resolvase should provide, and the data are more consistent with, two centers of hydroxyl radical generation symmetrically placed above (or in) the major grooves to each side of the cross-over point. The most relevant data are the following: (i) the overall distribution of cleavages

is relatively broader than that with S10C (that is, the outer cleavages are relatively more intense suggesting that the hydroxyl radicals are generated further from the center of the site); (ii) when data for both strands are normalized, cleavage at +7 (bottom strand) [directly across the major groove from +2 (top strand)] is of about equal efficiency to that at +3 (top strand), suggesting that the hydroxyl radical source is equidistant from the +3 and +7 positions and closer to the +2 and +1 positions; this would place the source in the major groove as indicated in Figure 6. Interpretation of the K65C data is relatively straightforward. The most efficiently cleaved sites (+3, top strand; –3, bottom strand) are not immediately across a groove from one another and so are likely to result from distinct but symmetrically placed centers of hydroxyl radical generation. Significant cleavages are visible across the major groove from each of the primary cleavages (e.g., at +9, +10 bottom strand), suggestive of a major groove location for the source of hydroxyl radicals but very close to the primary cleavage sites.

If the cluster of foci shown in Figure 6 is approximately correct and corresponds to the position of the side chains of residues 10, 65, and 72, it should mirror the arrangement of these residues on the surface of the protein. Here we are making the assumptions that (i) the statistical position of highest hydroxyl radical concentration is very close to the derivatized side chain and (ii) the derivatization has not affected the conformation of the protein or the protein–DNA complex in any major way. In the crystal structure of the N-terminal domain, residues 10, 65, and 72 form an approximately equilateral triangle on the catalytic surface, with the positions in clockwise order (Sanderson et al., 1990). Translated onto the DNA surface, this should convert to a triangle with the positions in counterclockwise order. The centers of hydroxyl radical generation form three different pairs of nonoverlapping triangles, all with the predicted counterclockwise order—10, 65, 72 (the relevant residues in a dimer of resolvase form two nonoverlapping triangles). However, only one of the three is consistent with the 1,2 dimeric arrangement of monomers that we have shown binds to an individual site I (Hughes et al., 1993). The dyad of the 1,2 dimer intersects the plane of the triangle to form a quadrilateral with the clockwise order of positions—10, 65, dyad, 72. By looking at the surface of the DNA and assuming that the dyads of the 1,2 dimer and site I coincide, the three hydroxyl radical centers and the DNA dyad should then form a quadrilateral with the reverse (i.e., counterclockwise) order. The only cluster of foci that fulfill this prediction is shown outlined in Figure 6. If this deduction is correct, the 1,2 dimer of the N-terminal domain is oriented with its long axis approximately perpendicular to the helical axis of the DNA (see Figure 7).

This alignment of the 1,2 dimer not only places the active site regions of the protein close to the cross-over site as our data suggest but also accounts for the lack of site-specific DNA cleavage at site I by the modified K29C and E102C mutants. For both of these modified mutants, the derivatized residues are on a surface of the catalytic domain that does not appear to interact directly with the *res* DNA at site I. Glu-102 is right at the 1,2 dimer interface but lies in the region furthest from DNA in the model. Moreover, the center of site I would be masked from hydroxyl radicals generated around residue 102 by the body of the resolvase dimer. The Lys-29 residues are located at opposite ends of the 1,2 dimer and in the model, as with Glu-102, are separated from DNA by the bulk of the protein.

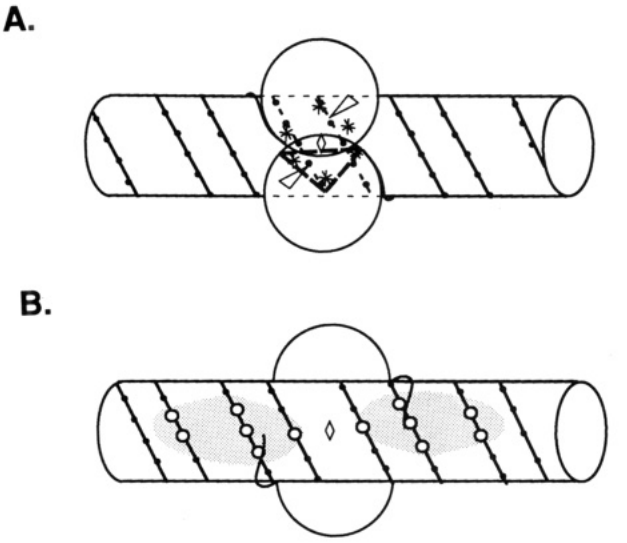

FIGURE 7: Model for resolvase binding at site I of *res*. (A) View looking down the dyad of the resolvase 1,2 dimer (overlapping circles) through the protein onto the minor groove containing the dyad of site I. Asterisks represent the approximate positions of the modified residues as determined from the site-specific DNA cleavages (see Discussion). Black dots represent the phosphates of the sugar–phosphate backbone. (B) View from opposite face of the DNA. The curved lines crossing the helix into the C-terminal domain binding sites represent the "hinge" regions of a resolvase dimer—a portion of the protein that is thought to be responsible for positioning the C-terminal domains with respect to the DNA binding sites. The shaded areas with open circles represent the regions contacted by the C-terminal domain of resolvase. The diamond symbols in the major and minor grooves indicate the dyad axis of the binding site.

Since the Ser-10 residues of the 1,2 dimer observed crystallographically are too far apart to allow interaction with an undistorted cross-over point, it seems likely that binding to site I is accompanied both by an unwinding of the center of site I, increasing the distance between cleavage sites, and by an adjustment of the 1,2 dimer (perhaps a scissor-like movement of the two interacting α helices [P. Rice, and T. Steitz, manuscript in preparation]) to swing the two active sites closer together. Both adjustments may be effected by tension between the N- and C-terminal domains of each resolvase monomer since, in B-DNA, the C-terminal DNA binding domain would have to wrap around the DNA helix to reach its binding sites located on the opposite face from the cross-over site. Protein flexibility accommodating the binding of ligands is known to occur for other proteins (Anderson et al., 1990; Faber & Matthews, 1990), and for a dimer of Cro protein, DNA binding induces a large conformational change at the dimer interface (Brennan et al., 1990; Caruthers et al., 1990).

Asymmetric Interactions between Resolvase and Binding Sites II and III. Resolvase must interact differently with each binding site in *res*. The variability in spacer length changes the geometry of each site placing the C-terminal domain binding sites, at site I, on one face of a B-DNA helix, while at sites II and III, the sites are displaced angularly from one another. Since the geometries of the resolvase binding sites are unique, it is not surprising to find that the derivatized mutants produce different DNA cleavage patterns at each site in *res*. More surprising, however, was the clear asymmetry in the cleavage patterns resulting from the EDTA derivatives of both S10C and D72C bound to sites II and III. This was in marked contrast to the symmetrical cleavages observed at site I. The asymmetries are of two types (see Figure 5). Predominant cleavages were observed mainly within the left half of both sites, and those cleavages that were detectable

within the right half were asymmetrically positioned relative to the center of the site, being shifted either to the right of site II or to the left of site III. Neither with S10C nor with D72C did the cleavages fall clearly into two clusters. This, together with the asymmetry, makes it unclear whether the cleavages result largely from a single source of hydroxyl radicals (the second source being more distant and perhaps more shielded from the DNA) or from two sources, asymmetrically positioned relative to the dyad sites. The asymmetry was accentuated by the results with the derivatized E102C which cleaved exclusively within the left half of site II and the right half of site III. Since the two Glu-102 residues lie very close to the dyad of the 1,2 dimer (the E102C mutant readily forms a covalent disulfide-linked dimer), it was particularly surprising to find efficient cleavages so far from the dyad of each DNA site. Presumably the lack of symmetrical interaction between resolvase and either site II or site III results from asymmetries in the nucleotide sequences of these sites. An obvious candidate in site II is the dA_6 tract which is likely to encourage asymmetric deformation of the center of site II. Other possibilities include the differences in the strength of the interaction between the resolvase C-terminal domain and each half of a site; the bendability of the DNA sequences within and between the binding sequences (Travers, 1991); and possible base-specific interactions between the N-terminal domain and the DNA which, for reasons of sequence asymmetry, are confined to half of a binding site. Whether the asymmetry we have observed here is of relevance to the structure and function of the synaptic complex remains to be seen.

ACKNOWLEDGMENT

We thank Phoebe Rice and Tom Steitz for invaluable discussions and help with computer graphics. We thank Robert Hughes, Christian Parker, Earl May and Catherine Joyce for reading the manuscript and helpful discussions. We thank the W.M. Keck Foundation Biotechnology Resource Laboratory (Yale University) for analysis of the derivatized proteins. Finally we thank Kate Tatham for help in preparation of the manuscript.

REFERENCES

Abdel-Mequid, S. S., Grindley, N. D. F., Templeton, N. S., & Steitz, T. A. (1984) *Proc. Natl. Acad. Sci. U.S.A. 81*, 2002–2005.

Anderson, B. F., Baker, H. M., Norris, G. E., Rumball, S. V., & Baker, E. N. (1990) *Nature 344*, 784–787.

Brennan, R. G., Roderick, S. L., Takeda, Y., & Matthews, B. W. (1990) *Proc. Natl. Acad. Sci. U.S.A. 87*, 8165–8169.

Bruice, T. W., Wise, J., & Sigman, D. S. (1990) *Biochemistry 29*, 2185.

Chen, C.-H. B., & Sigman, D. S. (1987) *Science 237*, 1197–1201.

Dervan, P. (1991) *Methods Enzymol. 208*, 497–515.

Dixon, W. J., Hayes, J. J., Levin, J. R., Weidner, M. F., Dombroski, B. A., & Tullius, T. D. (1991) *Methods Enzymol. 208*, 380–413.

Dröge, P., Hatfull, G. F., Grindley, N. D. F., & Cozzarelli, N. R. (1990) *Proc. Natl. Acad. Sci. U.S.A. 87*, 5336–5340.

Ebright, R. H., Ebright, Y. W., Pendergrast, S. P., & Gunasekera, A. (1990) *Proc. Natl. Acad. Sci. U.S.A. 87*, 2882–2886.

Ebright, Y. W., Chen, Y., Pendergrast, P. S., & Ebright, R. H. (1992) *Biochemistry 31*, 10664–10670.

Echols, H. (1986) *Science 233*, 1050–1056.

Echols, H. (1990) *J. Biol. Chem. 265*, 14697–14700.

Ermácora, M. R., Delfino, J. M., Cuenoud, B., Schepartz, A., & Fox, R. O. (1992) *Proc. Natl. Acad. Sci. U.S.A. 89*, 6383–6387.

Faber, H. R., & Matthews, B. W. (1990) *Nature 348*, 263–266.

Graham, K. S., & Dervan, P. B. (1990) *J. Biol. Chem. 265*, 16534–16540.

Grindley, N. D. F., Lauth, M. R., Wells, R. G., Wityk, R. J., Salvo, J. J., & Reed, R. R. (1982) *Cell 30*, 19–27.

Hatfull, G. F., & Grindley, N. D. F. (1986) *Proc. Natl. Acad. Sci. U.S.A. 83*, 5429–5433.

Hatfull, G. F., & Grindley, N. D. F. (1988) in *Genetic Recombination* (Kucherlapati, R., & Smith, G. R., Eds.) pp 357–396, American Society for Microbiology, Washington, D.C.

Hatfull, G. F., Noble, S. M., & Grindley, N. D. F. (1987) *Cell 49*, 103–110.

Hatfull, G. F., Sanderson, M. R., Freemont, P. S., Raccuia, P. R., Grindley, N. D. F., & Steitz, T. A. (1989) *J. Mol. Biol. 208*, 661–667.

Hirs, C. H. W. (1967) *Methods Enzymol. 11*, 197–199.

Hubbard, A. J., Bracco, L. P., Eisenbeis, S. J., Gayle, R. B., Beaton, G., & Caruthers, M. H. (1990) *Biochemistry 29*, 9241–9249.

Hughes, R. E., Hatfull, G. F., Rice, P. A., Steitz, T. A., & Grindley, N. D. F. (1990) *Cell 63*, 1331–1338.

Hughes, R. E., Rice, P. A., Steitz, T. A., & Grindley, N. D. F. (1993) *EMBO J.* (in press).

Kuwabara, M. D., Yoon, C., Goyne, T., Thederahn, T., & Sigman D. S. (1986) *Biochemistry 26*, 7234–38.

Landy, A. (1989) *Annu. Rev. Biochem. 58*, 913–949.

Lührmann, R. (1988) in *Structure and Function of Major and Minor Small Nuclear Ribonucleoprotein Particles* (Birnstiel, M. L., Ed.) pp 71–99, Springer, Berlin.

Mack, D. P., Sluka, J. P., Shin, J. A., Griffin, J. H., Simon, M. I., & Dervan, P. B. (1990) *Biochemistry 29*, 6561–6567.

Maxam, A., & Gilbert, W. (1980) *Methods Enzymol. 65*, 499–560.

Moore, S., & Stein, W. H. (1963) *Methods Enzymol. 6*, 819–831.

Mizuuchi, K. (1992) *Annu. Rev. Biochemistry 61*, 1011–1051.

Noller, H. F. (1991) *Annu. Rev. Biochem. 60*, 191–227.

Oakley, M. G., & Dervan, P. B. (1990) *Science 248*, 847–850.

Reed, R. R. (1981) *Cell 25*, 713–719.

Reed, R. R., & Grindley, N. D. F. (1981) *Cell 25*, 721–728.

Reed, R. R., & Moser, C. D. (1984) *Cold Spring Harbor Symp. Quant. Biol. 49*, 245–249.

Rimphanitchayakit, V., & Grindley, N. D. F. (1990) *EMBO J. 9*, 719–725.

Rimphanitchayakit, V., Hatfull, G. F., & Grindley, N. D. F. (1989) *Nucleic Acids Res. 9*, 1035–1050.

Salvo, J. J., & Grindley, N. D. F. (1988) *EMBO J. 7*, 3609–3616.

Sanderson, M. R., Freemont, P. S., Rice, P. A., Goldman, A., Hatfull, G. F., Grindley, N. D. F., & Steitz, T. A. (1990) *Cell 63*, 1323–1329.

Sigman, D. S. (1986) *Acc. Chem. Res. 19*, 180–86.

Sigman, D. S., Kuwabara, M. D., Chen, B., & Bruice, T. W. (1991) *Methods Enzymol. 208*, 414–433.

Sluka, J. P., Horvath, S. J., Bruist, M. J., Simon, M. I., & Dervan, P. B. (1987) *Science 238*, 1129–1132.

Sluka, J. P., Griffin, J. H., Mack, D. P., & Dervan, P. B. (1990a) *J. Am. Chem. Soc. 112*, 6369–6374.

Sluka, J. P., Horvath, S. J., Glasgow, A. C., Simon, M. I., & Dervan, P. B. (1990b) *Biochemistry 29*, 6551–6561.

Travers, A. A. (1991) *Curr. Opin. Struct. Biol. 1*, 114–122.

Tullius, T. D. (1989) *Annu. Rev. Biophys. Biophys. Chem. 18*, 213–37.

Williams, K. R., & Konigsberg, W. H. (1991) *Methods Enzymol. 208*, 516–539.